CHAPTER 3 METHODOLOGY & APPARATUS

The experimental study described in this dissertation focuses on absolute coverage measurements of adsorbed alkali-metal submonolayers on semiconductor surfaces by Rutherford Backscattering Spectrometry (RBS) performed in ultrahigh vacuum (UHV). Direct absolute coverage measurements by RBS have the ability to confirm or refute conclusions based on theoretically-predicted structural models, experimentally-observed structures, or relative coverage measurements obtained by alternative surface science techniques.

The general protocol for these RBS experiments can be described in three steps: (1) to produce a clean sample that it is contaminant-free as determined by various surface science diagnostic probes; (2) to perform the actual RBS coverage measurements (including calibration); and (3) to analyze the RBS data using ion scattering spectrometry simulation software.

A schematic of the experimental chamber is shown in Figure 3.1. The chamber is attached to a 0.5 - 2 MeV ion beam line and is equipped with an ion energy detector; a goniometer on which to mount, anneal, and precisely position the sample with respect to the ion beam; Auger Electron Spectroscopy (AES) and Low Energy Electron Diffraction (LEED) systems for surface diagnostics; and a getter source to prepare the alkali-metal adsorbate layers. Besides the energy detector in the vacuum chamber, the RBS system

includes the ion accelerator, beamline, beam source detector, ion detector, and electronics data acquisition software and hardware.

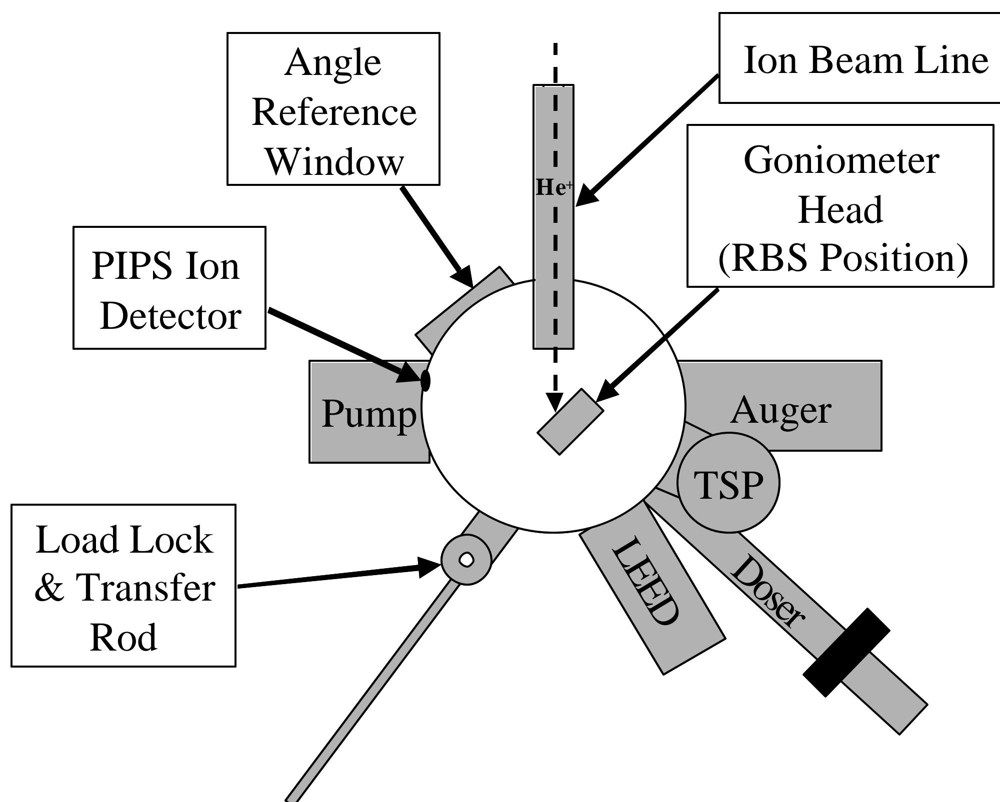

Figure 3.1. An overhead view of the experimental chamber.

3.1 Overview of Rutherford Backscattering Spectrometry

Bøgh first proposed the application of ion scattering as a surface probe in 1965.[1] There are numerous experimental approaches to ion scattering that have been developed since then, from which RBS has prevailed as a particularly useful technique for surface and thin film analysis. This technique can analyze the elemental composition as a function of depth in the near-surface region by taking advantage of the well-understood

Rutherford scattering cross section for an energetic ion beam interacting with atoms in a solid under pure electrical repulsion between the ion and atomic nuclei.[2]

In order to model an ion and the nucleus of an atom in a solid as the Coulombic interaction between point particles, the influence of the electrons around the atomic nucleus and the nuclear interaction force should be small. The electrons only significantly shield the nuclei beyond about 0.1 Å (1 Å = 1 Angstrom = 10^{-10} m). The nuclear force has an effective range of just a few fm (1 fm = 1 femtometer = 10^{-15} m). A simple calculation shows that a helium ion must have a kinetic energy in the 50 keV - 3 MeV range for its closest approach to a target nucleus to be within the screening electron cloud for a head-on collision. The data in this work were collected with a ~500 keV beam energies, the lowest energy at which the accelerator produced acceptable current. A low beam energy of ~500 keV was chosen for two reasons: (1) minimize penetration by the ions because the near-surface region is the area of interest and (2) scattering cross-section for Cs increases at lower energies. In this energy range, the differential Rutherford scattering cross section, $\frac{d\boldsymbol{s}}{d\Omega}$, (in the lab frame of reference) is given by:

$$\frac{d\boldsymbol{s}}{d\Omega}=\left(\frac{z_1 z_2 e^2}{2E_I \sin^2(\boldsymbol{f})}\right)^2 \frac{\left(\sqrt{1-\frac{m_1}{m_2}\sin(\boldsymbol{f})}+\cos(\boldsymbol{f})\right)^2}{\sqrt{1-\left(\frac{m_1}{m_2}\sin(\boldsymbol{f})\right)^2}}$$

Equation 3-1

where m_1, z_1 and m_2, z_2 are the atomic numbers and masses, respectively, of the two nuclei, e is the elementary unit charge, E_I is the incoming ion energy, and ϕ is the scattering angle[3]. Typical units of the scattering cross section are cm^2/streridian.

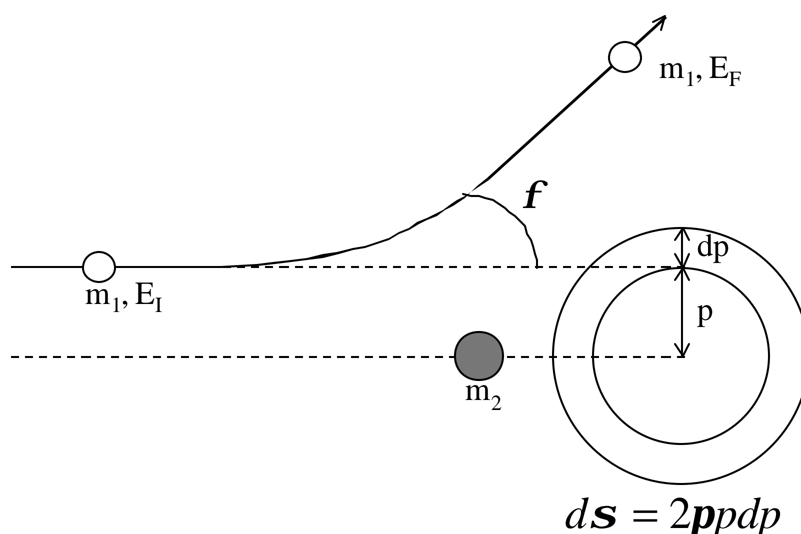

Figure 3.2 Scattering geometry for RBS.

Small corrections to the Rutherford cross-section for electron screening and possible nuclear resonances can be included using numerous approximations (see Tesmer and Nastasi[2] for details). A commercial software package, in our case, RUMP[4] (see below for discussion), is used to simulate the spectral data and determine absolute elemental density as a function of depth.

A collimated, monoenergetic ion beam from an accelerator (see Section 3.8) is incident on a material and the scattering angles and recoil energies of these ions are measured. When an incoming ion is incident upon a target nucleus and the energy is sufficiently large that the electronic forces holding the target atom in place are negligible, the collision can be analyzed straightforwardly using conservation of energy and momentum. The final energy, E_F of a scattered ion of mass m_1 and initial energy E_I that collides with a nucleus of mass m_2 and scatters through an angle ϕ, is given by[2]

$$E_F = E_I \left(\frac{\sqrt{m_2{}^2 - m_1{}^2 \sin 2(\phi)} + m_1 \cos(\phi)}{m_1 + m_2} \right)^2$$ **Equation 3-2**

The energy and cross-section equations are the basis of the analysis of masses and areal densities (surface coverages) of elements in the surface region. The number of recoiling ions detected at a given energy and angle is counted and summed up as a number C to compute the areal density of the target nucleus associated with that recoil energy. The areal density is generally written (N · t), where N is the number of nuclei per unit volume, and t is the thickness of a given slab of material. (N · t) for a target nucleus of a given mass is then given by

$$(N \cdot t)_i = \frac{C_i \cos(\phi)}{Q \Omega \sigma_i (E_I, \phi)}$$ **Equation 3-3**

where Q is the number of incident ions, and σ_i is the average of the Rutherford cross section for the target nucleus taken over the small solid angle Ω of the detector.[2]

Although the interaction of the ion with the electrons of the target nucleus can be ignored when analyzing the primary scattering collision, electron-ion interactions as the ion penetrates into the bulk are significant and must be considered in the analysis. As the ion travels through the sample, energy is imparted to the electrons as well. These collisions are also described by the Rutherford scattering formula (Eq. 3-1)with increasing cross-section as the ion energy decreases. Thus, an ion penetrating a sample loses energy more rapidly at larger depths. The net result is that the spectrum of ions recoiling from a single element target has a sudden onset below some critical energy, and then, for lower energies, the number of ions recoiling steadily increases.

Analysis of data from samples with lighter elements that than the substrate can be complicated by the fact that an ion that recoils from a heavy nucleus buried deep in the sample can emerge with the same energy as an ion that recoils from a light nucleus at the surface of the sample. For Cs/Si experiments, however, this is not a problem, since the heavy cesium ions reside on the surface, and the bulk is entirely made up of lighter silicon atoms. RBS Spectra look like the sample spectrum in Figure 3.3. Absolute cesium coverages are determined by comparing the area of the peak at E_{Cs} with the area of the Si scattering continuum properly accounting for ion-electron interactions in the bulk.

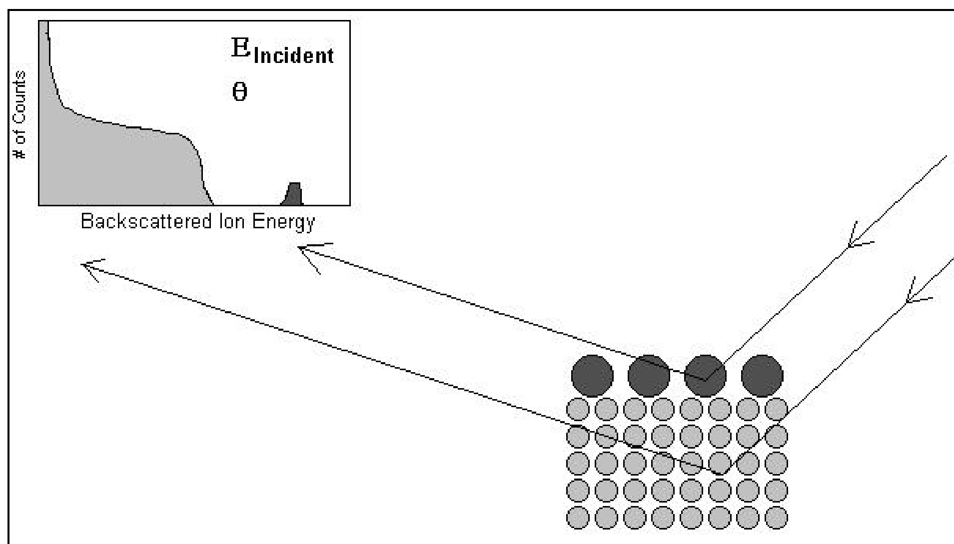

Figure 3.3 Helium ions incident on a sample. A few scatter from heavier Cs atoms (large circles) on the surface layer and recoil with energy, E_{Cs}. Others scatter from the Si atoms at the surface and in the bulk (small circles) and recoil in a continuum with an onset at $E_{Si} < E_{Cs}$.

The analysis above is based on the assumption that the likelihood of any collision of an ion with a nucleus is independent of any collisions with other nuclei. In the ideal case, the energy of a detected recoiling particle corresponds to a unique depth for a given element due to a single collision event. This however may not always be the case, it is also possible in principle to have a low particle recoil energy that is caused not by deep penetration of the sample but by multiple collisions. There is an increased probability of such events at low energies because of increased scattering cross-section and increased population of less energetic ions at larger depths. The standard simulation package used does not compute these complex effects and as a result at low energies, there is a tendency for the experimentally obtained counts to be higher that those of the simulation.

Another effect to consider is channeling. If the nuclei of the crystal target, are lined up one behind the other (e.g., the beam is aligned with one of the crystallographic axes) then the ions are much more likely to hit the surface ions. The ions, which do not collide with surface atoms are actually guided along the crystallographic rows by the electrons in the system largely avoiding nuclei below. This effect is called channeling.[5] Generally speaking, a 500KeV beam of helium ions must be within 2° of a major crystallographic axis for channeling to occur.[2] The experiments reported here were performed off any channeling axes.

3.2 Summary of experimental procedures

The rough outline of the ideal experimental procedure is as follows. A polished silicon wafer is cut to expose a given face. It is then introduced into an ultrahigh vacuum environment (in practice, we achieve a base pressure of ~10^{-10} torr). An electrical current is run through the sample for annealing to flash off the oxide layer on the silicon surface, formed during exposure to air. The electrical current is slowly reduced, allowing the cleaned surface to relax to its stable configuration. The wafer is then checked making use of AES and LEED. AES is a surface sensitive probe, used to detect chemical species. What is relevant to our studies is that the sensitivity near the surface layers is good enough to detect impurities at concentrations as low as one percent. Similarly LEED is also a surface sensitive probe and gives a good idea of the long-range order and structure of the surface. Together the probes verify the overall quality of the surface. After going

through AES and LEED, cesium is dosed onto the sample from an electrically-heated cesium chromate source (which emits pure cesium). The sample is dosed in steps, to put down incremental layers of cesium. The Auger signal is monitored to measure coverage. Dosing is stopped when the Cs signal strength reaches a constant value indicating that saturation has been achieved. Then LEED is again used to verify that the final surface symmetry is the desired one. After these preliminary steps the main RBS experiment is conducted followed by analysis of data to obtain the absolute coverage measurement.

In practice, every time LEED or Auger is performed on the sample or when cesium is deposited, the motion of sample or the cesium source causes pressure bursts. To avoid undue contamination, no single sample used in the actual experiment undergoes the full range of tests as described above. Generally, numerous preliminary measurements are made using test samples and performing AES and LEED to determine the proper sample preparation procedure and ensure its repeatability. Thereafter, any sample studied with RBS has only minimal verifications of purity made to minimize contamination.

3.3 Vacuum System

The general requirement for high-quality surface science studies on reactive surfaces is that the surface remains atomically clean over the duration of an experiment. Thus experiments are routinely performed in an ultrahigh vacuum ($<10^{-9}$ torr) environment. Roughly, at a pressure of 10^{-6} torr, gas atoms impinge upon a sample surface at a rate of

one atom per surface atom per second. If every impinging gas atom were to stick to a surface atom (sticking probability of unity), the sample surface would be completely contaminated in one second. In ultrahigh vacuum, say at a pressure of 10^{-10} torr, the pressure at which most of our experiments are carried out, each surface atom is struck every ~10000 sec (~3 h). Less reactive surfaces have low sticking coefficients so the sample might be expected to remain clean for up to a day, but measurements on more reactive surfaces can only span a few hours.

The chamber used for these experiments utilizes standard UHV components and UHV-compatible materials. The pumping system is comprised of series turbomolecular pumps (Leybold-Heraeus Turbovac 340-M backed by a Turbovac-50 and evacuated by a standard mechanical roughing pump) and a LN_2-cooled titanium sublimation pump.

Pressure measurements are carried out with Granville–Phillips nude ion gauges. Because the filament emits both electrons and light, the must be turned off whenever LEED or RBS measurements are made so as not to interfere with viewing (LEED) or the ion detector (RBS). The ion gauge is located away from either of the pumps in the chamber so that vacuum readings will accurately represent the pressure in the main chamber.

For sample introduction without breaking vacuum, the system is equipped with a small load-lock chamber, independently pumped by a turbomolecular pumping system, and a sample transfer rod that slides a sample held in a sample holder in to or out of the main vacuum chamber.

During the course of an experiment, pressure bursts and gas loads due movement of components in the vacuum (such as sample transfer) and degassing are kept to a minimum. When the sample and holder are first placed in the chamber, they are annealed one to two days for outgassing. For cleaning, sample flash anneals are performed over brief intervals so that the pressure is maintained at $<4\times10^{-9}$ torr; for the final flash, the pressure is $<1\times10^{-9}$ torr. Alkali-metal getter sources are continuously outgassed from new and are flashed before samples are introduced. For alkali-metal depositions, clean dosers caused pressure increases of only $\sim6\times10^{-11}$ torr. There is only a slight increase in pressure by $\sim1 \times 10^{-10}$ torr when the main vacuum chamber is open to the ion beamline.

3.4 Sample Manipulator / Goniometer

The sample is mounted on a goniometer[6] that allows for translational positioning on a horizontal plane, rotational positioning about a vertical axis, and tilt. Precise positioning is required to set channeling directions. The schematic of the laser alignment system shown in Figure 3.4 is used to determine the position of the sample normal for initial sample alignment.

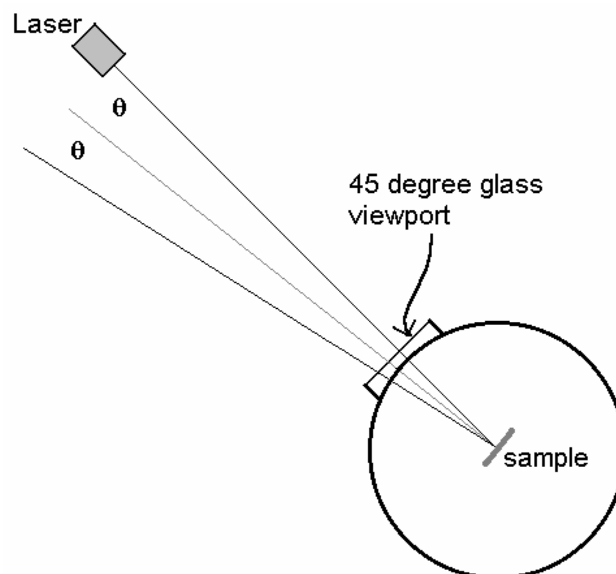

Figure 3.4 The laser sample positioning geometry. The laser beam enters the chamber through centering crosshairs on the 45° view port, hits the sample, and reflects back at an angle 2q, where q is the angle between the incoming beam and the sample normal.

The laser beam spot from the incident and reflected ray to the sample are made to coincide with the centered crosshairs on the 45° viewport to assure that the laser beam and the sample normal are exactly at 45° with respect to the incident ion beam. The tilt angle is measured in a similar way using the displacement of the reflected laser spot from the crosshair in the vertical direction.

3.5 Auger Electron Spectroscopy (AES)

Auger electron spectroscopy (AES),[7] is a technique for identifying the relative concentrations of elements in the near-surface region of a sample. A beam of 3-10 keV

electrons is directed toward the sample. In the Auger emission process, incident electrons create core holes. One radiation-less mechanism for the atom to relax is to fill the core hole with a valence electron and, in order to conserve energy and momentum, for another electron to be ejected. The energy of the Auger electron is derived from the energies of three electronic states of the target atom given a distinct elemental signature. Since the relative sensitivities to different elements are known[8] for a 3keV incident electron beam, it is possible to calculate relative coverages. Since many other scattered electrons are also detected by the analyzer, the Auger contributions are typically small features on a large background. Therefore, Auger spectra are typically analyzed reported as derivative spectra, dN/dE vs. E where E is the kinetic energy of the analyzed electron.

This technique is particularly well-suited to surface experiments because electrons in this kinetic energy range have a mean free path[9] of about 30 Å. Electrons that travel farther than the mean free path is likely to be scattered making the probe highly surface sensitive.

A Physical Electronics Model 15-110 Cylindrical Mirror Auger Electron Spectrometer is used in these experiments. The electron energy spectrum is differentiated as it is collected using a lock-in amplifier to enhance the Auger peaks from the background. A dN/dE vs, E spectrum is recorded on an x-y plotter.

In an AES experiment, the electron beam is focused on the surface for quite some time while the energy range of interest is scanned. The steady energetic electron bombardment and marginal outgassing of the Auger apparatus during operation can cause

surface contamination.[10] Typically only specific spectral regions of interest are scanned to minimize the length of time collecting Auger spectra.

3.6 Low Energy Electron Diffraction (LEED)

The phenomenon of electron diffraction from crystalline lattices was discoverd by Davisson and Germer.[11] LEED is a probe, which takes advantage of this phenomenon to characterize surfaces. As with AES, the low mean free path of electrons in this energy range (about 100 eV, for LEED) means that the probe is highly surface-specific.

The LEED system is essentially just an electron gun with a phosphorescent viewing screen positioned to receive diffracted electrons from the sample surface, which form a diffraction pattern with spots. Because these spots depend on the constructive interference of the signal from many different atoms in the surface, they will only be sharp if the surface is well-ordered. Again, the LEED electron beam can cause surface contamination and the order of experiments is carefully selected and time minimized.

3.7 Sample Preparation and Cesium Dosing

There are two or three stages to sample preparation for the experiment reported in this work: (1) prepare a clean silicon surface, (2) *for alkali-metal adsorption on a Si(111)($\sqrt{3}\times\sqrt{3}$)-R30°B surface template*: prepare a B-induced surface reconstruction by deposition of decaborane ($B_{10}H_{14}$), (3) deposit an alkali-metal adsorbate layer.

3.7-a Silicon Preparation

The silicon samples are 7×21 mm rectangles cut from thin polished commercially-produced wafers.[12] The Si(100) wafers are p type (boron doped) with a restivity of ~5 Ωcm and the Si(111) wafers are n type(Phosphorous doped) with a resistivity of ~4 Ωcm. The sample is cleaned in acetone and mounted into a sample holder, which secures it with two molybdenum clamps. The clamps are connected to two pins on the back of the sample holder for a series electrical connection for annealing and to detect current incident on the sample from the various probes. The back of the sample holder is alumina, which is a high melting point electrical insulator.

The sample and holder are introduced into the main chamber via the load lock. The goniometer head has a mechanical support for the holder and two sockets which run through carefully coiled wires to electrical feedthroughs out of the chamber. Before experiments can be run it is necessary to degas the system. This is accomplished by running a 1 A current through the silicon sample.

Outgassing and annealing semiconducting samples such as Si by a series circuit requires a well-regulated power supply to first bring the sample into conduction and then to supply sufficient current to complete the anneal without severe transients. A Sorensen DCR 300-3B was used, which has a maximum voltage of 400 V and a maximum current of 5 A. Even in current-limited operation, however, the sample resistance can drop so rapidly that current spikes occur. To eliminate this problem, a series 1Ω 10 W ballast resistor is used. Initially, the sample and sample holder outgas significantly and it

typically takes up to two days to regain pressures in the 10^{-10} torr range. Over the course of outgassing, the goniometer head reaches a temperature of ~150°. When outgassing is completed, the oxide layer on the silicon surface remains undisturbed. At this point, the sample and goniometer are allowed to cool to room temperature. The surface oxide is removed by flash annealing the sample to ~1100°C requiring a high current. For the high current flash, the low current power supply is used to bring the sample into conduction and a 25 A Sorensen[13] power supply is connected with a switcher box incorporating a shunt to make a smooth transition. The complete sample anneal takes place as a series of four or so flashes each of ~20 s duration each at maximal current. (Between flashes, the sample is left in conduction with about 0.20 A running through it for periods of up to several minutes to allow the pressure to stabilize.) Each flash follows a specific procedure. Over 10 s, the current is ramped up to 2 A (any faster, and the power supply spikes up to an overload of 25 V). When a steady current of 2 A is achieved, the sample resistance is sufficiently low for the current to be increased freely. Over the next 5 seconds, the current is ramped up to the target value (usually 7-10 amps), and left there for the desired time (or until a maximal pressure is reached). The current is ramped down over 5 seconds to ~4 A (6 A) for the Si(111) 7×7 (Si(100) 2×1), and then ramped down over a minute or so to the resting current. The intermediate current of 4A(6A) is a little above where the pressure drops dramatically. This represents the point where crystallization occurs and must be passed through slowly. Generally, the maximum pressure during flashing is in the mid 10^{-9} torr range, and the maximum pressure on the

last flash is typically below 2×10^{-9} torr. Once the sample has been flashed, the goniometer temperature has generally climbed to about 90°C, so the system requires 2-3 hours to cool down. At that point, Auger and LEED scans typically show that clean surfaces with the appropriate structure. At this point, the sample is ready for further preparation.

3.7-b Boron Doping of Si(111)

For producing a boron-induced Si(111)($\sqrt{3}\times\sqrt{3}$)R30°–B reconstruction on a Si(111) surface, additional procedures for doping boron into the subsurface layer are followed subsequent to obtaining the clean silicon surface. A well-established external doping recipe for obtaining this surface was used.[14] A dosing apparatus consisting of a vial of decaborane ($B_{10}H_{14}$) was connected to the vacuum chamber by a leak valve on one side and a valve attached to a roughing pump on the other side.

The source of boron was decaborane, a toxic chemical which is a crystalline powder at room temperature. However decaborane sublimates quickly at 70°C at atmospheric pressure. It is necessary to ensure that the entire volume of the dosing apparatus is free of atmospheric gases and filled by decaborane. To do this, the dosing apparatus was first evacuated by the roughing pump. Subsequently the decaborane was heated above the sublimation point and the apparatus was pumped out several times. The repetition of this procedure ensures decreasing levels of atmospheric gases. A pressure gauge connected to the dosing apparatus monitored the gas pressure to check that there were no leaks and the dosing environment remained clean.

During an actual dose the decaborane was heated to ~100°C using heating tape and a hot air blower. The gas was released into the chamber in a controlled manner by the leak valve. The gas is delivered to the sample by a straight tube that runs from the leak valve right up to the sample surface. The chamber pressure was monitored to ensure a proper dosing environment.

3.7-c Cesium Dosing Procedure

The cesium layer is deposited using a commercial SAES[15] getter source, which is simply a small amount of cesium salt in a metal case with a small slit. An electrical current is run through the case, which heats it up and starts a chemical reaction, which emits cesium through the slit. The getter may expel other elements besides cesium, and therefore must be outgassed very extensively before clean samples can be prepared. New dosers are flashed annealed at 7 A for 30 s every 5 m and occasionally run at 5 A for 20 m intervals. These procedures are carried as frequently as possible until pressure bursts from doser are acceptable - pressure increase during dosing $<1 \times 10^{-10}$ torr at a current of 5 A. Even after annealing is completed, ~3 A or are continuously run through the doser to keep it clean and prevent readsorption of contaminants from the chamber environment.

The doser is mounted on a retractable rod, so it can brought to within ~2 cm of the sample while dosing. During a dose, the current through the doser is ramped up to the desired value over about ~15 s after a ~90 s warm-up period far from the sample. When

the dose is complete, the doser is retracted and then the current through it is slowly ramped down.

Since the rate of dosing varies from one doser to the next, each doser must have its deposition rate calibrated by an Auger uptake curve (shown in the next chapter), where the intensity of the cesium Auger peak is plotted as a function of dose time. As more cesium goes down on the sample, the cesium Auger intensity should steadily increase. When the layer saturates, however, no more cesium sticks, and the Auger intensity levels off. Thus when the graph of cesium intensity versus time flattens, saturation has been reached. (Generally the ratio of the cesium intensity to silicon intensity is used to eliminate possible systematic errors.)

3.8 Rutherford Backscattering Spectrometry (RBS) System

Once a saturation time has been established for a given doser, and the sample is found to have a clean Auger signal and the appropriate LEED pattern, the sample is ready for measurement of the absolute coverage via RBS. The RBS system consists of the accelerator the sample and the dectector.

3.8-a Accelerator

The accelerator is the heart of the RBS experiment because it is the source of the ion beam. The quality of the beam in terms of intensity, collimation and energy definition is crucial. For this work, the beam was generated by a National Electrostatics Corporation

5SDH tandem Van de Graaff generator with a radio frequency plasma ion source[16] shown schematically in Figure 3.5. Some of the basic components will be described.

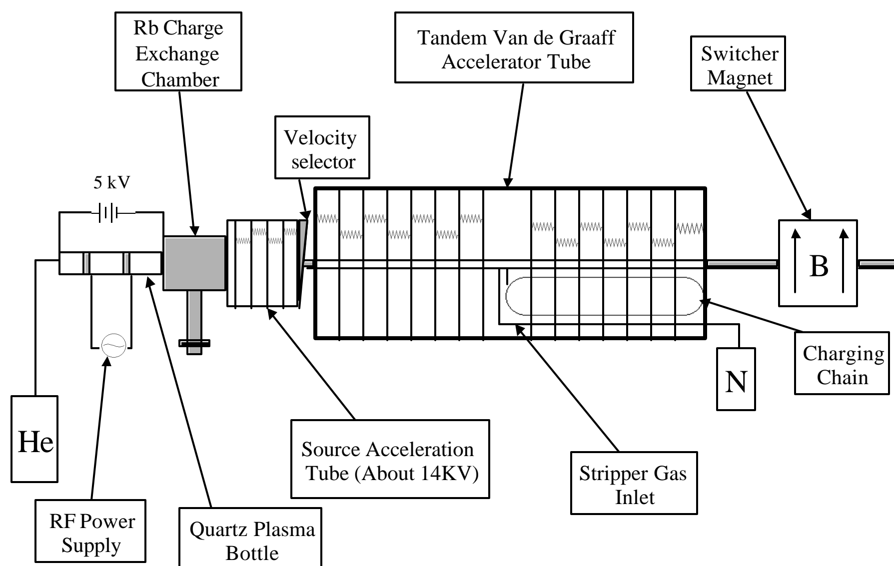

Figure 3.5 The NEC 5SDH tandem Van de Graaff accelerator.

The primary acceleration voltage is developed by a Van de Graaff generator, which consists of a pelletron chain consisting of small metallic segments connected via insulating links. The chain rotates, with one end at ground potential, where each segment is given a small positive charge as it goes by. At the other end of the chain exists the high voltage terminal. As each link passes this terminal, positive charge is deposited to build or maintain a large electric potential. The terminal voltage was generally ~243 kV for the experiments giving a ~500 keV $^{4}He^{+}$ beam was used. While lower energy beams are desirable for best increases sensitivity to ultrathin films at surfaces, this is the lowest energy at which the accelerator could produce sufficient beam current.

Helium ions are obtained by rf excitation of helium gas in a plasma container. An rf source creates a plasma and a 5 kV dc voltage extracts the positive He ions out of the plasma. Tandem accelerators require negative incoming ions for ideal operation so the He ions from the plasma tube are given a negative charge by passage through a rubidium vapor whereby the Rb atoms donate their single valence electron to the helium ions which emerge from the charge exchange chamber in a variety of charge states. The desired $^{4}He^{-}$ ions are extracted by acceleration through a small linear acceleration tube with about 14 kV across it and passage through a velocity selector, which deflects the beam by 3° so that the neutral particles as well as most of the undesired beam constituents are rejected. The $^{4}He^{-}$ ions then enter the tandem accelerator with an energy of ~18 keV. The negative ions are accelerated towards the positive terminal in the center of the accelerator after which they pass through low pressure N_2 which removes electrons from the ions converting many positive ions. These positive He ions are repelled by the positive terminal voltage and accelerate away from the center of the accelerator. In this way in two stages, the tandem accelerator can impart more kinetic energy to the ions than the maximum potential reached by the terminal. The energy imparted also depends on the charge combinations of the incoming and outgoing ions. For the He^{-} and $^{4}He^{+}$ ion combination, the kinetic energy is approximately double the maximum voltage reached by the positive central terminal. The $^{4}He^{+}$ ions are deflected 15° into the MEIS beam line via a switcher magnet with a vertical magnetic field. This field once again performs an effective mass selection and rejects any ions emerging from the accelerator besides the

$^4He^+$. The final He^+ kinetic energy is: 18 keV from the source plus 243 keV for the $^4He^+$ approaching the terminal plus 243 keV for the $^4He^+$ moving away from the terminal for a total of 504 keV. Actually, the energy is somewhat lower than this because the initial acceleration of the ions in the plasma is mostly shielded so the effective energy is generally 500 ± 1 keV for most runs.

3.8-b MEIS / RBS Beamline

The ion accelerator is connected to several beam lines and uses switcher magnet to steer the beam from one beam line to another. The beamline configuration for these experiments is illustrated in Figure 3.6. After the switcher magnet deflects the ions into the beamline, they are collimated and focused by a series of electrostatic lenses, magnetic lenses, and apertures. A Faraday cup is mounted in the middle of the beamline to monitor beam quality and provide feedback for beam focusing and adjustments.

The next portion of the beam line is the differential pumping and beam collimation section. The accelerator is a high vacuum system (pumped by two turbomolecular pumps, one at each end of the accelerator), but since the stripper gas is continuously leaked in during operation, its pressure is generally in the 10^{-6} torr range. In order to ensure that the MEIS chamber can operate at UHV with a pressure a factor 10^{-4} smaller than the beamline, a series of small conductance apertures and pumps are implemented in the beamline.

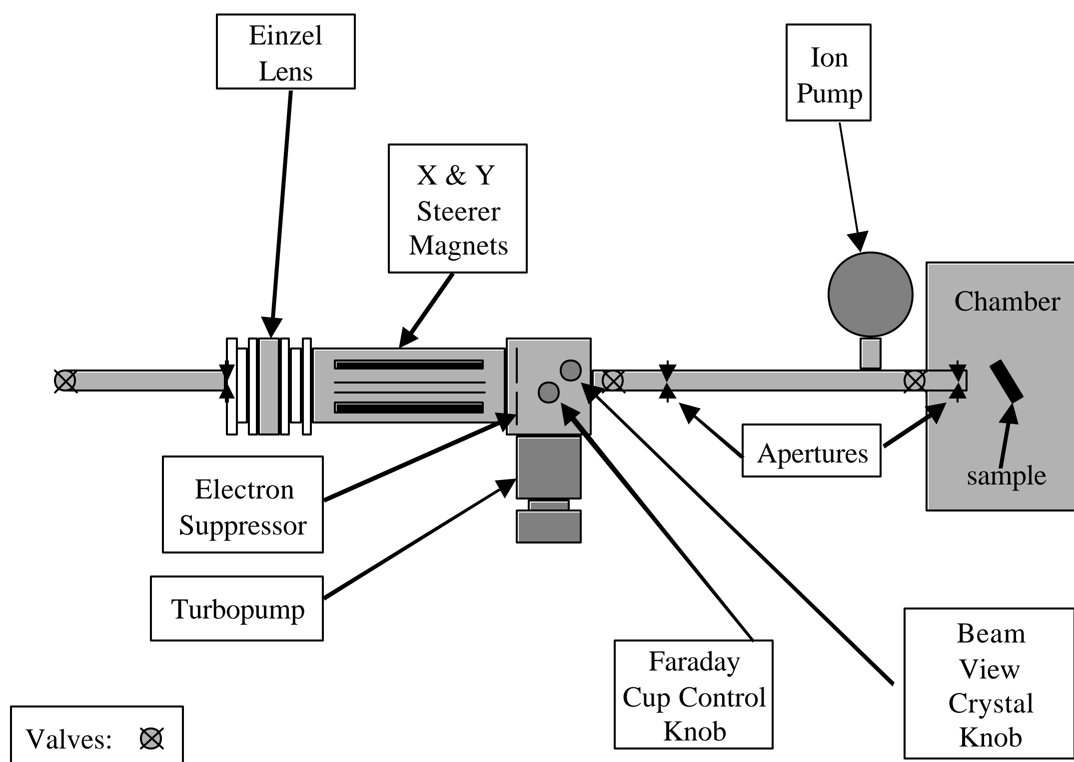

Figure 3.6 Beamline Schematic.

The first pump is a turbopump[17] which brings the pressure down into the 10^{-7} torr range. The beam then passes through a 9.322 mm diameter aperture and into a region, which is pumped by an ion pump[18] held in the 10^{-9} torr range. The final beam-defining aperture is actually inside the MEIS chamber itself and is 1.23 mm wide by 0.616 mm high. One more larger skimmer aperture, 1.984 mm in diameter, helps reduce gas conductance into the chamber and skim off electrons or ions, which pass through the earlier aperture at extreme angles. The effective collimation of the midline aperture (110.49 cm from the sample), and the final aperture (9 cm from the sample) gives 0.5°

beam spread at the sample. The differential pumping allows the MEIS chamber to be maintained in the low 10^{-10} torr range during RBS runs. Beam currents of 0.5-0.8 nA are typical.

The chamber is aligned with the beam by a series of positioning screws and bolts. It is fully free to move in three dimensions or to rotate as needed over a small range. The chamber is aligned so that the beam coming in through the final aperture (which is carefully machined to be centered) hits a crosshair on the beam window on the far side of the chamber. This assures that the beam runs directly through the center of the chamber.

3.8-c RBS Experiments

As Rutherford first observed in his early ion scattering experiments, when an ion beam actually hits a sample, the number of ions, which recoil due to nuclear collision, is very small (<1% in our energy regime). Most of the ions simply implant themselves a few micrometers into the target.

Besides the incident beam current, the beam ejects many secondary electrons from the sample. If no compensation is made, the flow of negative charge away from the sample can produce an error in beam current up to a factor of two. Biasing the sample at ~300 V relative to the walls of the chamber greatly reduces the escape of secondary electrons back to the sample.

In a RBS experiment, absolute coverage measurements require knowledge of the total dose on the sample (current integration). Since the beam current is ~1 nA, the 300 V sample bias can create small leakage currents if there is not almost perfect isolation.

Although the sample is mounted on an alumina ceramic base plate some leakage current still exists, which is compensated by a current offset box. Other current integration errors come from high-energy secondary electrons as well as x-rays that scatter from the walls of the chamber to send photoelectrons back to the sample. The net result is a current integration error on the order of 20%. For these experiments current integration corrections can be made quantitatively and reliably by fitting data from the silicon substrate to a RUMP simulation. Current integration and this consistency check allow reliable determination of the absolute Cs coverage.

The ion detector is a bakeable Canberra Passivated Implanted Planar Silicon (PIPS) detector; the diode operates at a reverse bias of 40 V. The detector has an active surface area of 25 mm^2 and is mounted on a flange directly at the wall of the chamber, which is 75° away from the beam line in a horizontal plane (θ), and 25° above the horizontal plane (ϕ). The signal from the detector is processed by a preamplifier connected directly to the outer wall of the chamber to reduce noise, an amplifier which outputs a pulse whose height is proportional to the energy of the detected ion an Analog-to-Digital Converter (ADC), and a multi-channel analyzer from which the data is fed to a computer. In detection, errors due to light leakage and pileup are minimized.

3.8-d RBS simulation and analysis (RUMP)

The data are saved in ASCII format and then imported into a commercial analysis package called RUMP.[4] Inputs to the RUMP program include beam energy; the ion species; integrated incident charge; detector solid angle; angles between the sample

normal, incoming beam and the ray from the beam spot to the sample detector; and energy resolution. At this point, RUMP can produce a simulation of the expected spectrum from, e.g., cesium on silicon for the specified conditions.

RUMP models the system as a series of slabs with areal densities and compositions, which the user enters. Elemental ratios are entered, and the areal density (or thickness) of each slab. For layers thicker than 100 Å (such as our silicon substrates), RUMP must be instructed to use sublayers of 100 Å or less, otherwise it produces highly distorted results (strong suppression of the near-surface count rate).

The calculated spectrum can be compared with the experimental spectrum and various features matched to get the scaling and normalization parameters. The scaling is associated with the correlation between the measured electrical pulse height that the detector electronics record, and the actual energy of the incident ion detected. There is a linear relationship between these quantities, so only two numbers are required to specify it. For our experiment, the leading edge of the silicon shoulder and the middle of the cesium peak both have energies which can be calculated and assigned to the observed channels. This provides sufficient information to set the channel to energy offset and scale, which RUMP requires. The final normalization is done by comparing the high energy end of the silicon spectra. The absolute height of the simulated and observed spectra should be the same in this region. By setting the correction factor appropriately, any errors in the charge integration can be accounted for (up to an uncertainty of about 3%). The result is a spectrum, which is calibrated rigorously to measure absolute

coverage of the cesium layer. The actual coverage determination is made, by varying the areal density of the simulated layer until the area under the simulated peak is identical to the area under the experimental peak.

One weakness of RUMP is that it does not take into account multiple scattering events, i.e. ions which have two or more collisions with nuclei before emerging from the sample. Generally, the multiple scattering cross-section is negligible. However, small deflections of the ion due to highly-shielded collisions with atoms are not negligible, and these deflections remove extra energy from the ion, and tend to make experimental spectra higher than their simulations at lower energies. The cross section for deflections greater than some critical angle θ_c is given by the integrated form of the Rutherford cross section:[2]

$$\sigma_c = 1.6\times10^{-26}\left(\frac{Z_1 Z_2}{E}\right)^2 \cot^2\left(\frac{\theta_c}{2}\right)$$

Equation 3-4

(where E is in MeV, and Z_1 and Z_2 are the atomic numbers). The units of the integrated cross section are cm^2 whereas the units of the differential cross section in 3-1 are cm^2 per solid angle. Moore[19] reported that for 1 MeV helium ions going through a slab of silicon with a total areal density of about 1.2×10^{19} atoms/cm^2, the simulations were generally about 3% low. The reported experiments were carried out at half that energy, which the above equation shows, should quadruple the cross section and cause at least a 16-fold increase in multiple scattering events [20]. As shall be seen subsequently, this is roughly in

keeping with experimental observations and supports the rationale to match RBS fits to the leading edge of the silicon shoulders.

One other factor, which RUMP calculations take into account, is straggling. This phenomenon is simply the spreading of energies of ions as a group of them goes through a target. It is a purely statistical process, relating to the fact that no two ions will have exactly the same interactions with the electrons in the substrate. Tesmer and Nastasi give an excellent discussion of how to make corrections for straggling.[2] Straggling effects are negligible or unobservable in our energy regime and scattering geometry, so most of the simulations here have ignored straggling effects.

A few words should be said here about experimental errors and how they affect the simulations. Fortunately, errors in measuring the solid angle of the detector or the integrated beam current can be accounted for by scaling the simulation to fit the silicon data. Errors in measuring the angles of the experiment, however, cannot be compensated for in such a direct manner.

The primary effect that angle error has is if the error is in estimating the angle between the sample normal and the incoming beam Θ. The amount of cesium the beam passes through is proportional to $1/\cos(\Theta)$. Thus the observed coverage is strongly dependent on Θ. Fortunately, Θ is measured relatively accurately – to within 2°, limited by the glare of the alignment laser. Since Θ is generally 45° for these experiments that means a 3.5% error in the measurements. If either of the other two angles involved in RUMP simulations is off, the significance is not so direct. The energy lost exiting the

sample changes, and that changes the shape of the spectrum a little, but the net effect is typically not so large. This type of angular uncertainty arises because the exact point on the sample where the beam is hitting is unknown. Since the sample is only 7 mm wide, and the detector is almost 300 mm away, this makes for an angular uncertainty of about 1°. Numerous simulations have shown that the combined effects of all angular errors is to introduce an uncertainty of ~5% to the coverage measurements.

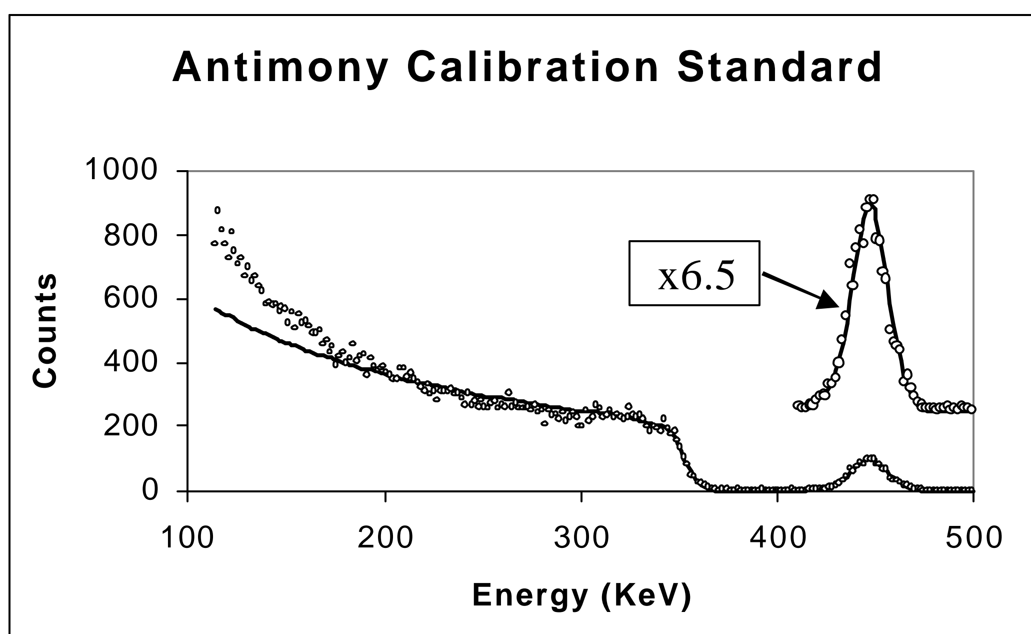

Figure 3.7 RBS spectrum (500 KeV, Θ = 45°) from an antimony doped calibration standard (circles), and the RUMP simulation (lines). The antimony peak is enlarged at right. The simulation which matches the data is for 97% of the actual amount of antimony in the sample.

An RBS spectrum of a well-defined sample is used to calibrate the system. The silicon wafer, which had been doped via ion implantation, had a known areal density of antimony in the near surface region.[21] The spectrum, along with the RUMP simulation is

shown in Figure 3.7. The fit to the antimony peak would predict 97% of the actual amount of antimony in the standard. Comparable accuracy can be expected in the values for the cesium coverages. Actually, since the cesium is known to be concentrated in a single layer at the surface of the silicon, the simulation should be more reliable than for the antimony sample, where the antimony is spread out over several hundred Angstroms.

List of References

[1] E. Bøgh, and E. Uggerhoj, Nucl. Instr. and Meth., **38**, 216 (1965).

[2] J. R. Tesmer, M. Nastasi, J. C. Barbour, C. J. Maggiore, and J. W. Mayer, *Handbook of Modern Ion Beam Materials Analysis* (Materials Research Society, Pittsburgh 1995).

[3] For a derivation of this, see E. Adams, Ph.D. dissertation, University of Pennsylvania, 1984, Appendix A.

[4] RUMP - RBS Analysis and Simulation Package [v. 4.00(beta)], (c) 1988-1997 Michael Thompson, Larry Doolittle, (c) 1988-1997 Computer Graphic Service, Ltd. All rights reserved, Revision Level: Version 0.950; L. R. Doolittle, Nucl. Instr. And Meth., B **9**, 5008 (1985).

[5] L. C. Feldman, J. W. Mayer, and S. T. Picraux, *Materials Analysis by Ion Channeling*, (Academic Press, New York,1982).

[6] Device for holding and moving a sample.

[7] P. Auger, J. Phys. Radium **6**, 205 (1925).

[8] L. E. Davis, N. C. MacDonald, P. W. Palmberg, G. E. Riach, and R. E. Weber. *Handbook of Auger Electron Spectroscopy, Second Edition*, (Physical Electronics Division, Perkin Elmer Corporation, Eden Prairie, Minnesota, 1978).

[9] A. Zangwill, *Physics at Surfaces*, (Cambridge University Press, Cambridge, 1988).

[10] Typically carbon and oxygen from the residual gasses in the chamber.

[11] C. J. Davisson, and L. H. Germer, Phys. Rev. **30**, 705 (1927).

[12] Si(111) wafers manufactured by Wacker-Chemitronic, GMBH; Si(100) wafers manufactured by Recticon Enterprises Inc., Pottstown, PA.

[13] Sorensen DCR 20-25B.

[14] I. W. Lyo, E. Kaxiras, and Ph. Avouris, Phys. Rev Lett. **63**, 1261(1990)

[15] SAES Getters, S.p.A., Lainate (Milano) Italy.

[16] In the Laboratory for Research on the Structure of Matter's Materials Characterization Facility.

[17] Leybold-Heraeus Turbovac-150.

[18] Varian Hi-Q Ion Pump.

[19] J. Moore, Nucl. Instr. and Meth. **174**, 577 (1980).

[20] W. Sherman, Ph.D. dissertation, university of Pennsylvania, 1999.

[21] Produced by AT&T, Murray Hill, NJ. Guaranteed 5×10^{15} Sb atoms/cm^2 $\pm$ 2%.